[10](a) R. K. Nesbet, Advan. Chem. Phys. 9, 321 (1965); (b) Phys. Rev. 155, 51 (1967); 155, 56 (1967); (c) 175, 2 (1968).
[11]H. F. Schaeffer, III, and F. E. Harris, Phys. Rev. 167, 67 (1968).
[12](a) O. Sinanoğlu and I. Öksüz, Phys. Rev. Letters 21, 507 (1968); (b) O. Sinanoğlu, Atomic Physics, edited by B. Bederson, V. W. Cohen, and F. M. J. Pichanick (Plenum Press, Inc., New York, 1969), p. 131; (c) N. R. Kestner, Chem. Phys. Letters (to be published).
[13]K. A. Brueckner, in Atomic Physics, Ref. 12b, p. 111.
[14](a) H. P. Kelly, Phys. Rev. 131, 684 (1963); (b) Advan. Theoret. Phys. 2, 75 (1968).
[15](a) K. A. Brueckner, Phys. Rev. 96, 508 (1954); (b) 97, 1353 (1968); (c) 100, 36 (1955).
[16]J. Goldstone, Proc. Roy. Soc. (London) A239, 267 (1957).
[17]J. C. Slater, Phys. Rev. 81, 385 (1951); see also Ref. 4.
[18]A. P. Yutsis, I. B. Levinson, and V. V. Vanagas, Mathematical Apparatus of the Theory of Angular Momenta (Israel Program of Scientific Translations, Jerusalem, 1962).
[19]J-N. Massot, E. El-Baz, and J. Lafoircriere, Rev. Mod. Phys. 39, 288 (1967).
[20]P. Nozières, Theory of Interacting Fermi Systems (W. A. Benjamin, Inc., New York, 1964), Chap. 6.
[21]J. C. Slater, Phys. Rev. 36, 57 (1930).
[22]C. E. Moore, Atomic Energy Levels (National Bureau of Standards, Washington, D.C., 1949), Vol. I.
[23]Recently, R. K. Nesbet, T. L. Barr, and E. R. Davidson [Chem. Phys. Letters (to be published)] obtained 105.2% of the experimental E_{corr} for the L-shell of Ne(^1S) using an extended basis. This supports our general conclusions.

PHYSICAL REVIEW A VOLUME 1, NUMBER 4 MARCH 1970

Semistatistical Model for Electrons in Atoms*

N. Ashby and M. A. Holzman
Department of Physics and Astrophysics, University of Colorado, Boulder, Colorado 80302
(Received 25 September 1969)

A simple modification of the Thomas-Fermi statistical model for electrons in atoms and ions is presented, which corrects one of the model's major deficiencies, namely, its overestimation of the electron density near the nucleus. Exploiting the fact that near the nucleus the potential is nearly Coulombic, boundary conditions are derived from wave mechanics and incorporated into the model equations. The resulting equations are expressed in integral form and solved by a straightforward iterative technique. Results for total atomic energies show marked improvement over the corresponding results obtained from the Thomas-Fermi model, with only a slight increase in the required computational effort. The procedure is extended to obtain a relativistic statistical model of the atom. Numerical results show good agreement with wave mechanics in total energy calculations and in the form of the density near the nucleus. The relativistic effects are of greater magnitude than exchange or inhomogeneity corrections to the Thomas-Fermi model for large Z atoms.

I. INTRODUCTION

Because accurate solutions of the Schrödinger equation for many-electron atoms are so difficult to obtain, it is of considerable interest to develop simplified models for the description of electrons in atoms.[1] This is particularly true if one is not interested in all the details of the electronic structure, but only in certain gross features such as, for example, an effective one-electron potential for use in calculations on single-particle excited states, for a description of the ion core potential in electron energy-band calculations in solids, or in certain moments of the electron charge density.

For these reasons the Thomas-Fermi (TF) model of the atom continues to attract widespread interest. This model is based on the crudest of approximations, namely, that the potential acting on the electrons may be replaced locally by a constant, and therefore that the electrons in a small volume element behave as "free" fermions, in a constant potential, with wave functions of the form $e^{i\vec{k}\cdot\vec{r}}$. This plane-wave approximation leads to a well-known expression for the kinetic energy density, which is proportional to the $\frac{5}{3}$ power of the electron density. Since the model electron density becomes infinite at the nucleus, the kinetic-energy density also becomes infinite, whereas from wave mechanics it is known that the electron density is constant, and that the kinetic-energy density approaches zero near the nucleus. This is perhaps the most serious defect of the TF model; among

other defects may be mentioned the facts that the electron density does not approach zero sufficiently rapidly for large radii and that no details of the electronic shell structure can be seen in the TF electron density. Consequently, results calculated from the TF model are rather disappointing except in a few specific cases.[1-3]

The problem of correcting the divergence of the kinetic energy density as $r \to 0$, that is, of obtaining the so-called "kinetic-energy correction," has been studied by a number of investigators.[4] In 1935, Weizsäcker[5] first derived a correction based upon the assumption that the wave functions of the electrons are modified plane waves of the form $(1+\vec{\alpha}\cdot\vec{r})e^{i\vec{k}\cdot\vec{r}}$, where α is a constant. A modified TF equation was derived which gives a constant electron density near the nucleus, in good agreement with the results of wave mechanical calculations. However, the agreement between energies is not correspondingly improved.[6] Recent work by Yonei and Tomishima[7] has shown empirically that if the Weizsäcker correction is reduced by the factor of $\frac{1}{5}$, then excellent agreement with wave mechanical energies is obtained.

The rigorous calculations of Kirzhnits,[8] Golden,[9] and Baraff and Borowitz[10] use perturbation expansions to obtain quantum corrections to the TF model in a formal way. Kirzhnits has shown that the factor by which the Weizsächer correction should be reduced is $\frac{1}{9}$. The work of Baraff and Borowitz is based on an expansion of the many-electron Green's function in a series in powers of $\hbar$; the lowest-order term gives the TF model. The next-higher-order terms arise from exchange and inhomogeneity effects. Schey and Schwartz[11] have studied these higher corrections by numerical methods and have shown that the corrected densities and potentials do not give significant improvement over the simple TF model; in some cases, poorer results are obtained. Thus, these attempts to improve the TF model have achieved only limited success; it is not clear whether improvements to the TF model have in fact been obtained.

Plaskett and March,[12,13] using a model adapted from application of the WKB approximation to the Schrödinger equation, included the centrifugal barrier in the potential. Greatly improved energies were obtained by replacing the factors $l(l+1)$ which occur in the wave equation by $(l+\frac{1}{2})^2$. This causes the radial density $4\pi r^2 n(r)$ to become zero at some inner cutoff radius. The presence of this inner cutoff, which reduces the normally high TF model density, is the principal reason why energies are improved in this model.

The purpose of this paper is to present a model for the atom which gives the correct form of the density near the nucleus in a natural way and which gives the correct form of the kinetic energy density in this region. The importance of obtaining such a model has been emphasized by Gombás.[4]

The model which we propose here is based on the observation that the TF approximation – treating the potential locally as a constant – is extremely poor very near the nucleus, precisely in the region where the model suffers from its most serious defect. But near the nucleus, the electron density is known to be approximately constant – the major contributions to the electron density in this region arise in wave mechanics from K-shell electrons, and for sufficiently small r the approximate form of the K-shell electron density can be easily obtained from wave mechanics.

The semistatistical model consists of retaining the TF model for radii r greater than some small radius r_0, but of using a wave-mechanical density $\rho_W(r)$ for radii $r < r_0$. From the density $\rho_W(r)$, boundary conditions on density, slope of the density, and on the kinetic energy density at r_0 (which are required to fit continuously on the corresponding quantities obtained from the TF model) equations for $r > r_0$ are obtained. In a sense, this patches up the TF model by building in wave mechanical information which is known to be relatively accurate for small radii. Because of the self-consistent manner in which the model equations must be solved, the modifications near the nucleus have the effect of slightly reducing the model density at large radii and result in a more realistic one-electron potential.

In Sec. II, we reformulate the TF equations in terms of an integral equation rather than a differential equation; the integral equation is much easier to solve numerically and allows in a simpler way for the inclusion of the semistatistical density for $r < r_0$. The integral equation also greatly simplifies the numerical solution (which is required for the calculation of effective one-electron potentials) of the TF equation for atoms of any degree of ionization. In Sec. III, the nonrelativistic semistatistical model is developed in detail and applied to the calculation of total atomic energies for selected ions.

The considerations leading to the semistatistical model may be easily extended to obtain an acceptable relativistic model of electrons in heavy atoms. They are discussed in Sec. IV.

II. INTEGRAL EQUATION FOR TF MODEL

In this section, we develop a method of solution of the TF model equations which increases the ease of obtaining self-consistent solutions for ions.

In Sec. III, this method of integration is used in the development of the semistatistical model, in which solution of the equations in differential form would pose extreme difficulties.

The basic equation of the TF theory for an atom or ion is [3,4]

$$\nabla^2\phi(r) = (4e/3\pi\hbar^3)\{2m[\mu - V(r)]\}^{3/2} - 4\pi Ze\delta(\vec{r}), \quad (1)$$

where $\phi(r) = -e^{-1}V(r)$ is the TF potential and μ is the Fermi energy (or chemical potential), which can be interpreted approximately as the minimum energy required to add another electron to the system. Solutions for the neutral atom ($\mu = 0$) are easily obtained in a straightforward way; however, it is not simple to obtain accurate solutions to this equation for positive ions ($\mu < 0$).[3,14] This is because the quantity $\mu - V(r)$, which appears on the right-hand side of Eq. (1), vanishes at some finite distance r_m from the nucleus; then the TF ionic potential is Coulombic past the point r_m, and the density of the core electrons vanishes at r_m. The difficulty is that the termination point r_m is determined through a condition on the value of the slope of the density that the desired solution is to have at r_m. This method is accurate for high degrees of ionization because the density curves cut the axis at a fairly large angle at r_m. For smaller degrees of ionization, the curves are nearly tangent at r_m; hence, the tangential slope and r_m cannot be accurately determined. Kobayashi[14] was able to remove this uncertainty in the solutions for ions of low degree of ionization by the adoption of a complex inward numerical-integration technique.

These solutions for TF ionic potentials can be accurately obtained if we choose not to use the differential form of Eq. (1) for the TF potential, but use instead an integral equation. The TF particle density is

$$n(r) = (3\pi^2\hbar^3)^{-1}\{2m[\mu - V(r)]\}^{3/2}. \quad (2)$$

Expressing the potential energy $V(r)$ in terms of the density gives

$$V(r) = -Ze^2/r + e^2\int d^3r'n(r')/|\vec{r} - \vec{r}'|.$$

Inserting this potential into Eq. (2) gives a self-consistent integral equation for the TF density,

$$n(r) = \frac{1}{3\pi^2\hbar^3}\left[2m\left(\mu + \frac{Ze^2}{r} - e^2\int\frac{d^3r'n(r')}{|\vec{r}' - \vec{r}'|}\right)\right]^{3/2}. \quad (3)$$

The solution $n(r)$ of this equation is subject to the boundary condition

$$\lim_{r\to 0} V(r) = -Ze^2/r + C, \quad (4)$$

where C is the constant potential at the nucleus due to the electrons, and the normalization condition

$$\int d^3r\, n(r) = N,$$

where N is the number of electrons. The parameter μ is adjusted to meet the normalization condition.

In order to facilitate numerical solution we take advantage of the assumed spherical symmetry of $n(r)$ and write

$$\int\frac{d^3r'n(r')}{|\vec{r} - \vec{r}'|} = \frac{1}{r}\int_0^r 4\pi r'^2 n(r')dr' - \int_0^r 4\pi r'n(r')dr' + \int_0^\infty 4\pi r'n(r')dr'. \quad (5)$$

Furthermore, we define the unitless quantities $\rho(x)$ and x by $r = a_0x$ and $\rho(x) = 4\pi a_0^3x^2n(x)$, where $a_0 = \hbar^2/me^2$ is the Bohr radius. Equation (3) can then be expressed in terms of the radial density $\rho(x)$:

$$\rho(x) = \frac{8\sqrt{2}}{3\pi}x^2\left[\xi + \frac{Z}{x} - \int_0^x\left(\frac{1}{x} - \frac{1}{x'}\right)\rho(x')\,dx'\right]^{3/2}, \quad (6)$$

where ξ is a constant defined by

$$\xi = \mu a_0/e^2 - \int_0^\infty [\rho(x')/x']dx'. \quad (7)$$

The definite integral in Eq. (7) represents the potential energy of an electron at the nucleus due to all the other electrons, and has been separated off so that the remaining terms in Eq. (6) depend only on values of the density at radii $x' < x$.

A method for integrating Eq. (6) is discussed in the Appendix. The method allows one to obtain numerically accurate self-consistent solutions for the density $\rho(x)$ for all degrees of ionization in a rapid manner. The procedure is to guess a value for ξ, integrate the density, and check for proper normalization. Normalization is achieved by adjusting ξ. The general behavior of the numerical solutions is illustrated in Fig. 1.

For the neutral case, in which the density is normalized to Z electrons, i.e.,

$$\int_0^\infty \rho(x)\,dx = Z, \quad (8)$$

the solution for $\rho(x)$ approaches the x axis asymptotically for large x and

$$\xi = -\int_0^\infty \rho(x)/x\,dx; \quad (9)$$

hence $\mu = 0$.

For ions, the argument in the brackets of Eq. (6) becomes negative beyond some value x_m, where $\rho(x_m) = 0$. This determines the cutoff for the ion density, i.e.,

$$0 = \mu a_0/e^2 + (Z - N)/x_m, \quad (10)$$

where $N < Z$ is the normalization of the density.

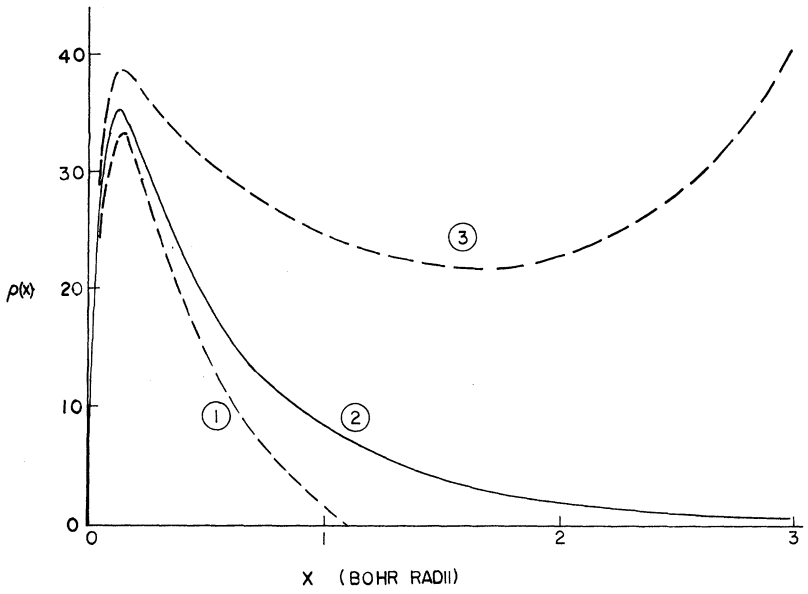

FIG. 1. The general behavior of the solutions to Eq. (6) as a function of ξ for $Z=29$: (1) $\xi<-160$, (2) $\xi=-159.82$ ($N=28$), and (3) $-160<\xi<0$.

Results of the numerical integration of Eq. (6) are presented in Table I. The values of the cutoff radius x_m for singly ionized atoms, as well as the density curves, agree with those of Brudner and Borowitz,[15] who use the integration technique of Kobayashi.

III. SEMISTATISTICAL-MODEL KINETIC-ENERGY CORRECTION

The well-known expression for the kinetic energy in the TF theory is easily obtained from the plane-wave approximation,

$$\mathrm{KE}=\frac{2}{(2\pi)^3}\int d^3r\int\frac{\hbar^2k^2}{2m}\,d^3k$$
$$=\int\frac{3h^2}{40m}\left(\frac{3}{\pi}\right)^{2/3}n(r)^{5/3}d^3r\equiv\int_0^\infty dx\,\epsilon_{\mathrm{TF}}(x). \quad (11)$$

We define here, in terms of the unitless quantities $\rho(x)$ and x, the radial kinetic-energy density $\epsilon_{\mathrm{TF}}(x)$ for the TF theory,

$$\epsilon_{\mathrm{TF}}(x)=\frac{e^2}{a_0}\left(\frac{243\pi^2}{2}\right)^{1/3}\frac{[\rho(x)]^{5/3}}{x^{4/3}}\,. \quad (12)$$

Figure 2 is a comparison of the TF radial density $\rho(x)$ and the self-consistent-field (SCF) wave-mechanical radial density near the nucleus. The TF model density approaches zero as $x^{1/2}$, whereas the wave-mechanical density approaches zero much more rapidly as x^2. More profound (see Figs. 3 and 4) are the comparisons in the TF and SCF theories between the respective kinetic-energy densities and between the functions $\rho(x)/x$ (which are the potential energy densities). In the TF theory these densities diverge. The comparisons clearly illustrate the gross deficiencies of the TF model for small radii.

We shall now show that the statistical density can be greatly improved without the use of the controversial Weizsäcker correction, but rather with a correction based on known approximate wave-mechanical results.

Near the nucleus, in the limit as $r\to 0$, the potential for any atom or ion behaves as follows:

$$\lim_{r\to 0} V(r)=-Ze^2/r+C\,, \quad (13)$$

where C is the constant potential at the nucleus due to all the electrons. Since we can easily solve the Schrödinger equation for a potential of form (13) to obtain the density, we can couple this wave-me-

TABLE I. Boundary radii and chemical potentials for various ions.

Ion	μ (eV)	x_m	x_m [a]
Li^+	−7.78	2.815	2.817
Na^+	−5.89	4.617	4.621
K^+	−5.23	5.199	5.204
Cu^+	−4.86	5.596	
Rb^+	−4.69	5.804	5.812
Ag^+	−4.54	5.997	
Cs^+	−4.46	6.120	6.127
Au^+	−4.27	6.380	
Fr^+	−4.24	6.434	

[a] See Ref. 15.

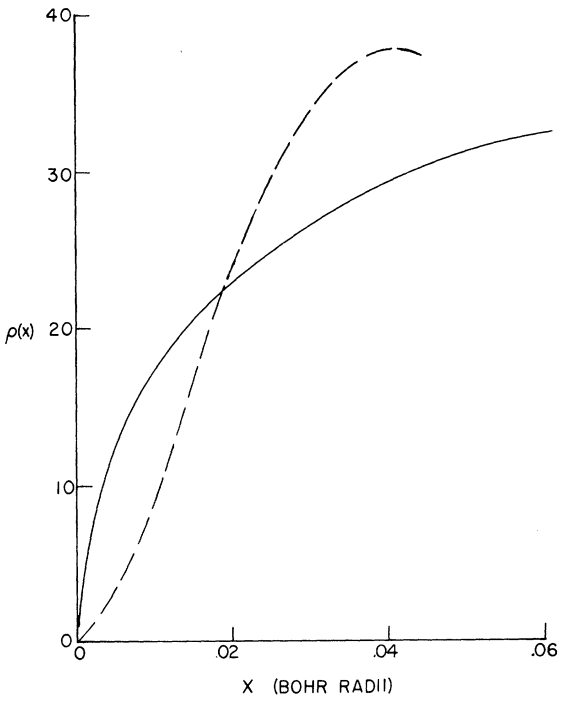

FIG. 2. Comparison of the TF radial density with that of the Hartree SCF for singly ionized copper. TF, solid line; Hartree, dashed line.

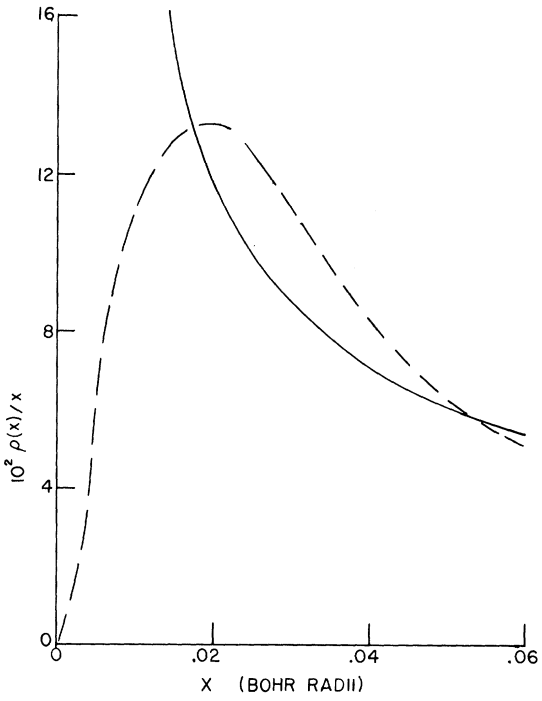

FIG. 4. Comparison of the TF and Hartree SCF potential-energy densities for singly ionized copper. TF, solid line; Hartree, dashed line.

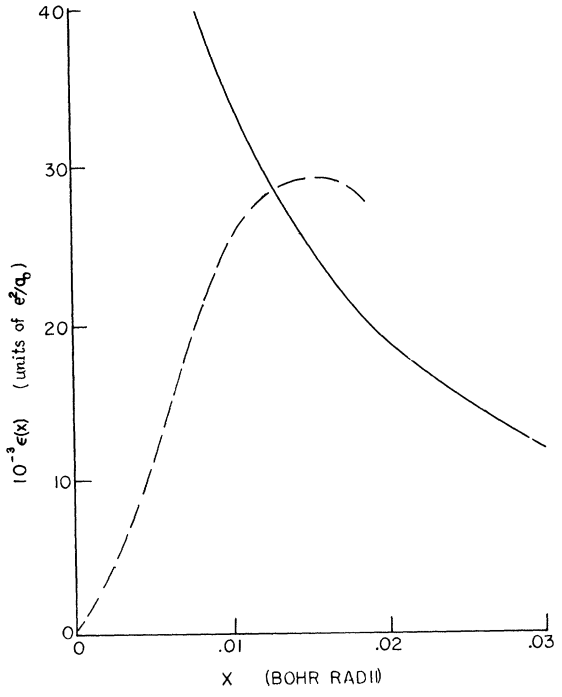

FIG. 3. Comparison of the TF and Hartree SCF kinetic-energy densities for singly ionized copper. TF, solid line; Hartree dashed line.

chanical density to the TF density in order to give the correct behavior for the density near the origin. As a first approximation, we shall assume that very close to the nucleus, for x less than some radius x_0 which is not yet specified, the density is due to electrons in the K shell only. By examination of the wave functions, one may see that this is a moderately good assumption because the next most significant contribution to the density is due to $2s$ electrons, which contribute less than 12.5% to the density. Hence, from the form of the K-shell wave functions in the Hartree approximation, we may expect, approximately,

$$\rho_W(x) = \alpha x^2 e^{-\beta x}, \quad x < x_0, \tag{14}$$

for the radial density. Here, α and β are constants which are yet to be determined.

The TF equation (6) for the density is assumed to be valid for $x > x_0$, and may be written as

$$\rho_{TF}(x) = \frac{8\sqrt{2}}{3\pi} x^2 \left[\xi' + \frac{1}{x}(Z - Z_W) - \int_{x_0}^{x} \left(\frac{1}{x} - \frac{1}{x'}\right) \rho_{TF}(x')dx'\right]^{3/2}, \quad (x > x_0) \tag{15}$$

where $\xi' = \xi + \int_0^{x_0} [\rho_W(x')/x'] dx'$,

$$Z_W = \int_0^{x_0} \rho_W(x')\, dx', \tag{16}$$

and x_0 is the boundary between the inner and outer regions where the wave-mechanical [Eq. (14)] and TF [Eq. (15)] densities apply, respectively. In Eq. (15), the radial integral has been broken into two pieces, one extending between the limits 0 and x_0 in which the wave-mechanical density appears, and one from x_0 to x in which the TF density appears. The integrals in ξ' and Z_W represent the contributions to potential and normalization from the inner region. The constant potential at the nucleus is

$$C \equiv e^2 \int_0^{\infty} [\rho(x)/x] dx,$$

where $\rho(x) \equiv \rho_W$, $x < x_0$

$\rho(x) \equiv \rho_{TF}$, $x > x_0$

and hence is uniquely determined by the self-consistent solution for the density $\rho(x)$.

In order to determine α, β, and ξ we use the following procedure. Because wave functions and their first derivatives are continuous, it is natural to assume that the density and its slope are continuous. Hence, it is necessary to specify the density and its slope at the initial point x_0 of the integration. We obtain these boundary conditions in terms of α and β from the wave-mechanical form, Eq. (14). Therefore, at x_0 we have from Eqs. (14) and (15)

$$\rho_{TF}(x_0) = \rho_W(x_0); \quad \frac{d\rho_W(x_0)}{dx} = \frac{d\rho_{TF}(x_0)}{dx}, \tag{17}$$

$$\frac{1}{\rho_W(x_0)} \frac{d\rho_W(x_0)}{dx} = \frac{2}{x_0} - \beta, \tag{18}$$

$$\frac{1}{\rho_{TF}(x_0)} \frac{d\rho_{TF}(x_0)}{dx} = \frac{2}{x_0} - \frac{3}{2} \left(\frac{8\sqrt{2}}{3\pi}\right)^{2/3} \times [x_0 \rho_{TF}(x_0)]^{-2/3} (Z - Z_W). \tag{19}$$

Equating (18) and (19) and using (17), we find

$$\beta = \frac{3}{2} \frac{(Z - Z_W)}{x_0^2 [\xi' + (Z - Z_W)/x_0]}. \tag{20}$$

Furthermore, from Eq. (17) we have

$$\alpha = [\rho(x_0)/x_0^2] e^{\beta x_0}. \tag{21}$$

The numerical technique is the following: Guess x_0, Z_W, and ξ', then integrate the TF density from x_0 to infinity while adjusting ξ' to achieve the proper normalization for the remaining $N - Z_W$ electrons:

$$\int_{x_0}^{\infty} \rho_{TF}\, dx = N - Z_W.$$

β and α are then determined from Eqs. (20) and (21). Since $\rho_W(x)$ is now determined [from Eq. (14)], it is checked to see if it is a solution to the second of Eqs. (16), i.e., that a consistent value of Z_W is obtained. If it is not, guess another value of Z_W and repeat the procedure until all conditions are satisfied for the chosen x_0.

In order to determine the boundary point x_0, we note that the radial kinetic-energy density due to the K electrons near the nucleus is

$$\epsilon_W(x) = -(\hbar^2/m) \psi_K^*(x) \nabla^2 \psi_K(x), \tag{22}$$

where the assumed form of the wave function is from Eq. (14):

$$\psi_K(x) = \left(\frac{\alpha}{8\pi}\right)^{1/2} e^{-\beta x/2}.$$

Hence, $\epsilon_W(x) = (e^2/a_0)(\beta/2x - \beta^2/8) \rho_W(x)$. (23)

We choose x_0 to be the point where the kinetic-energy density [Eq. (23)] fits continuously to the TF kinetic-energy density [Eq. (12)]. This corresponds in a sense to requiring second derivatives of the wave function to remain continuous. Thus, by requiring

$$\epsilon_{TF}(x_0) = \epsilon_W(x_0), \tag{24}$$

we uniquely determine the matching point x_0. If Eq. (24) is not satisfied, another value for x_0 is chosen and the calculation is repeated. The entire iterative procedure converges very rapidly.

In Figs. 5–7, the density $\rho(x)$, the kinetic-energy density $\epsilon(x)$, and potential energy density $\rho(x)/x$ are plotted for the copper ion Cu^+ near the nucleus. The improvement of the semistatistical method over the TF model, in comparison to the wave-mechanical approach, is clearly displayed. In Table II, results from the semistatistical model are compared to the TF and Hartree SCF treatments of the alkali ions and the related subgroup of copper, silver, and gold. SCF results are from calculations by Snow *et al.*[16] and by Dickinson.[17] The TF and semistatistical results are calculated using the numerical techniques described in this

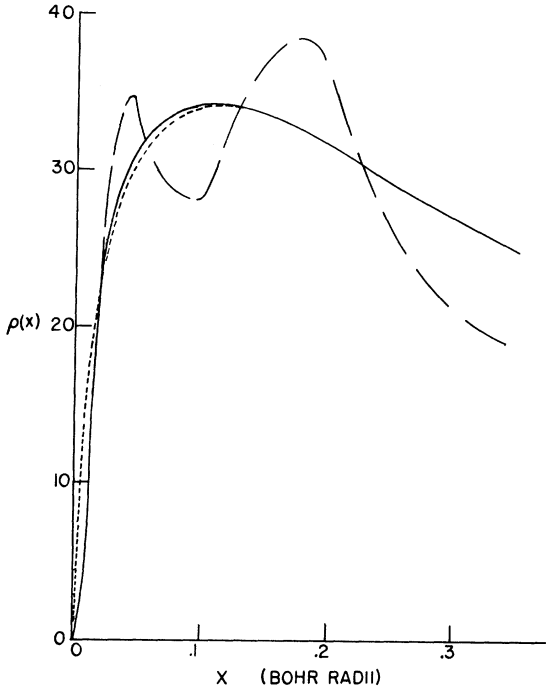

FIG. 5. Comparison of the nonrelativistic semistatistical (SS) TF, and Hartree SCF radial densities for singly ionized copper. SS, solid line; TF, short dashed line; Hartree, long dashed line.

work.

A characteristic of the solutions to the present model is that the boundary point x_0 increases rapidly for smaller Z. In fact, it is not possible to find

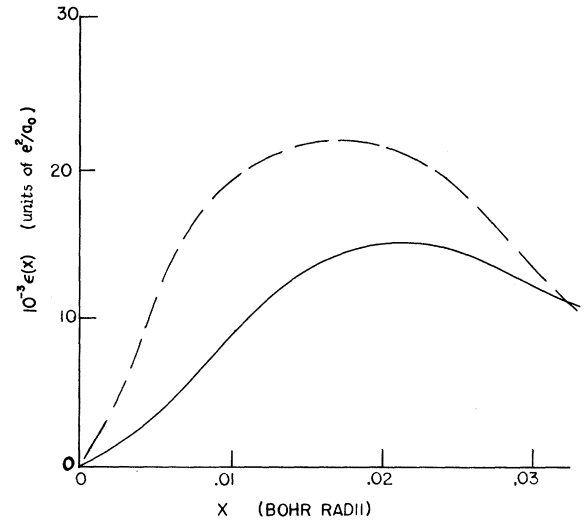

FIG. 6. The nonrelativistic semistatistical kinetic-energy density for singly ionized copper. $x_0 = 0.032$. $\epsilon_{TF}(x)$, solid line; $\epsilon_W(x)$, dashed line. (See Fig. 3.)

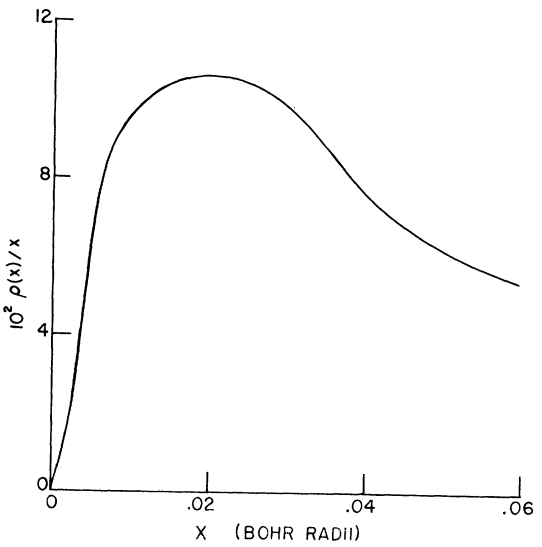

FIG. 7. The nonrelativistic semistatistical potential-energy density for singly ionized copper. (See Fig. 4.)

a point of intersection of $\epsilon_W(x)$ and $\epsilon_{TF}(x)$ for Li^+. This is to be expected because Li^+ consists only of K electrons, hence, the function $\rho_W(x)$ is the desired solution over the entire region.

The potential at the nucleus,

$$V_e(0) = \int_0^\infty [\rho(x)/x]\,dx\,, \tag{25}$$

when calculated from the TF model (when compared to the wave-mechanical result) is too large by 16% for large Z to 25% for smaller Z. When calculated by the present model, we see that it varies, respectively, from 3 to 14% too large. It is to be expected that the results should be better for larger Z, where the statistical model is more applicable.

The total energies in the semistatistical model are improved considerably over the TF results. If we calculate the total energy using the wave-mechanical kinetic-energy density [Eq. (30)] up to x_0 and the statistical kinetic energy density [Eq. (18)] beyond x_0, we find that the nonrelativistic energies are too high by 6% for large Z to 18% for Na^+. This cuts the error roughly in half over that attained in the TF model. If one assumes that the semistatistical density is a corrected statistical density such that all physical quantities are calculated strictly from formulas of the TF statistical theory, there is further improvement in total energy calculations. In this case, the energies are low by 1.5% for large Z to 1.5% high for Na^+, as compared to nonrelativistic SCF energies.

Barnes and Cowan[18] have calculated atomic binding energies based on cutting off the radial density at some inner radius. The advantage of the present approach is that good energies are obtained

TABLE II. Specific results from the Thomas-Fermi nonrelativistic and semistatistical models, and the Hartree SCF. All energies are in keV.

	TF		SCF		Semistatistical			
Z	$v_e(0)$	$-E$	$v_e(0)$ [a]	$-E$ [b]	$v_e(0)$	$-E_T$ [c]	$-E_W$ [d]	x_0
87	691.8	701.9		611.4	586.2	623.05	573.6	0.0098
79	608.3	560.3		486.03	512.3	495.32	454.7	0.0108
55	375.1	240.6	323	205.63	308.2	208.96	189.5	0.0159
47	304.3	166.83	262	141.5	246.9	143.56	129.44	0.0189
37	221.2	95.4	187.5	80.02	175.7	80.94	72.28	0.0245
29	159.7	54.05	133.5	44.65	124.0	45.08	39.86	0.0320
19	90.8	20.15	73.91	16.34	67.2	16.23	14.06	0.0515
11	43.7	5.62	34.8	4.42	29.8	4.28	3.59	0.0978
3	7.6	0.268	5.3	0.203				

[a] See Ref. 17. $v_e(0)$ is the potential at the nucleus due to the electrons.

[b] See Ref. 16.

[c] This energy is calculated using the expression $\epsilon_{TF}(x)$ for $x < x_0$ [Eq. (12)].

[d] This energy is calculated using the expression $\epsilon_W(x)$ for $x < x_0$ [Eq. (23)].

along with basic improvement in other properties, such as radial density, effective potential at the nucleus, etc., without the use of *ad hoc* cutoffs. Furthermore, this approach is directly applicable to the relativistic case which we shall now discuss.

IV. RELATIVISTIC SEMISTATISTICAL MODEL OF THE ATOM

The nonrelativistic relation

$$\hbar^2 k_f^2(r)/2m - V(r) = \mu \,, \tag{26}$$

which determines the maximum momentum an electron can have in the TF model, forces $k_f(r)$ to approach infinity near the nucleus. This reflects the fact that innermost electrons can have very large velocities and hence, especially for heavy atoms, relativistic-mass corrections are important. A relativistic relation corresponding to the above can easily be written by analogy as

$$[\hbar^2 c^2 k_f^2(r) + m^2 c^4]^{1/2} - V(r) = \mu_R = \mu + mc^2 \,, \tag{27}$$

which leads to a relativistic statistical density of the form

$$n(r) = (3\pi^2 c^3 \hbar^3)^{-1} \{[\mu_R - V(r)]^2 - m^2 c^4\}^{3/2} . \tag{28}$$

As r approaches zero, this statistical density becomes singular. The singularity is much worse than in the nonrelativistic case – here the density is nonintegrable. Rudjkobing[19] and Gilvarry[20] attempted to surmount this difficulty by developing a model based on a second-order form of the Dirac equation studied by Temple.[21] This equation is obtained by assuming that the potential is Coulombic in a small interval about r. The resulting statistical density is

$$n(r) = (3\pi^2 c^3 \hbar^3)^{-1} \times \left[[\mu_R - V(r)]^2 - m^2 c^4 - \left(r \frac{dV}{dr} \right)^2 \right]^{3/2} \tag{29}$$

and has been discussed by Gilvarry. The additional term $[r(dV/dr)]^2$ removes the nonintegrable singularity at $r = 0$, and the density then approaches zero as $r^{1/2}$, just as in the nonrelativistic model. This statistical density will therefore have the defects of the nonrelativistic model in this region.

The model of Plaskett[12] is obtained from the Klein-Gordon equation; the density divergence is still present but is eliminated by replacing the factor $l(l+1)$ by $(l+\frac{1}{2})^2$ in the centrifugal term of the effective potential. This introduces an inner cutoff in the radial density.

Just as in the nonrelativistic case, these difficulties may be surmounted by using the known wave-mechanical density for small radii. We assume that the radial density near the nucleus is of the approximate form

$$\rho_{RW}(x) = C x^{2\gamma} e^{-\beta x} \,, \tag{30}$$

where $\gamma = (1 - \beta^2 \alpha^2/4)^{1/2}$,

$\alpha = \hbar^2/me^2$ is the fine structure constant, and C and β are constants.

Equation (22) is obtained from the known form of the Dirac-Coulomb 1s wave functions which for spin-up is

$$\psi_K(x) = Dx^{\gamma-1}e^{-(\beta/2)x}\begin{bmatrix} 1 \\ 0 \\ i[(1-\gamma)/(1+\gamma)]^{1/2} & \cos\theta \\ i[(1-\gamma)/(1+\gamma)]^{1/2} & \sin\theta\, e^{i\phi} \end{bmatrix}, \tag{31}$$

where D is a normalization constant.[22]

As in Sec. III, the relativistic semistatistical radial density for $x > x_0$ is represented by the statistical form, obtained from Eq. (28) or (29). We shall develop here a relativistic model based on Eq. (28); the advantages of a corresponding model based on Eq. (29) will be discussed in Sec. V. By defining $\mu_R = \mu + mc^2$,[23] we obtain, from Eq. (28),

$$\rho_{RT}(x) = \frac{8\sqrt{2}}{3\pi}x^2\left[f(\xi', x) + \frac{\alpha^2}{2}f^2(\xi', x)\right]^{3/2}, \tag{32}$$

where

$$f(\xi', x) = \xi' + \frac{Z - Z_{RW}}{x} - \int_{x_0}^{x}\left(\frac{1}{x} - \frac{1}{x'}\right)\rho_{RT}(x')\,dx'. \tag{33}$$

In Eq. (33),

$$Z_{RW} = \int_0^{x_0}\rho_{RW}(x)\,dx .$$

We solve Eq. (32) by integrating from the point x_0, with initial conditions specified by continuity of the density and slope of the density:

$$d\rho_{RT}(x_0)/dx = (2\gamma/x_0 - \beta)\rho_{RW}(x_0), \tag{34}$$

$$\rho_{RT}(x_0) = \rho_{RW}(x_0) , \tag{35}$$

where

$$\frac{d\rho_{RT}(x_0)}{dx} = \frac{2}{x_0}\rho_{RT}(x_0) - \frac{3}{2}\left(\frac{8\sqrt{2}}{3\pi}\right)^{2/3} \times\left(\frac{\rho_{RT}(x_0)}{x_0^2}\right)^{1/3}(Z - Z_{RW}) \times\left[1 + \alpha^2\left(\xi' + \frac{Z - Z_{RW}}{x_0}\right)\right]. \tag{36}$$

From Eqs. (34) and (36) it is straightforward to solve for β,

$$\beta = \left\{\frac{Gx_0^2}{2} - x_0 + \left[x_0^2 + \alpha^2 G x_0\left(1 - \frac{Gx_0}{4}\right)\right]^{1/2}\right\}\frac{2}{x_0^2 + \alpha^2} , \tag{37}$$

where

$$G = \frac{3}{2}\frac{(Z - Z_{RW})}{x_0^2[\xi' + (Z - Z_{RW})/x_0]} \times\frac{1 + \alpha^2[\xi' + (Z - Z_{RW})/x_0]}{1 + \frac{1}{2}\alpha^2[\xi' + (Z - Z_{RW})/x_0]} . \tag{38}$$

It then follows that Eq. (35) uniquely determines C:

$$C = \rho_{RT}(x_0)e^{\beta x_0}/x_0^{2\gamma} . \tag{39}$$

The iterative method for solution of the density is identical to that discussed in Sec. III.

In order to determine a unique boundary point x_0, we again require continuity of the kinetic-energy density functions. The wave-mechanical radial kinetic-energy density is determined from

$$\epsilon_{RW}(x) = 2\times 4\pi x^2\int d\Omega\,\psi_K^*[C\vec{\alpha}\cdot\vec{p} + mc^2(\beta - 1)]\psi_K , \tag{40}$$

where the wave function is specified by Eq. (31).[24] The factor of 2 accounts for both K electrons. Evaluation of Eq. (40) gives

$$\epsilon_{RW}(x) = [2mc^2a/(1+a^2)]\rho_{RW}(x)(\alpha/x - a) , \tag{41}$$

where $a = [(1-\gamma)/(1+\gamma)]^{1/2}$.

The kinetic energy of the relativistic statistical density is obtained from the statistical phase-space density

$$\epsilon_{RT}(r) = 4\pi r^2\frac{2}{(2\pi)^3}\int d^3k\,[(c^2\hbar^2k^2 + m^2c^4)^{1/2} - mc^2] . \tag{42}$$

When expressed in the units of Eq. (41), Eq. (42) becomes

$$\epsilon_{RT}(x) = \frac{4x^2mc^2}{\pi\alpha^3}\int_0^{\alpha k_f(x)} y^2\,dy[(1+y^2)^{1/2} - 1], \tag{43}$$

where $k_f(x)$ is determined from Eq. (27). Hence,

$$k_f(x) = [(3\pi/4x^2)\rho_{RT}(x)]^{1/3} . \tag{44}$$

Integration of Eq. (43) gives

$$\epsilon_{RT}(x) = (x^2mc^2/\pi\alpha^2)([1 + \alpha^2k_f^2(x)]^{1/2} \times[k_f^3(x) + (1/2\alpha^2)k_f(x)] - (1/2\alpha^3)\ln\{\alpha k_f(x) + [1 + \alpha^2k_f^2(x)]^{1/2}\}). \tag{45}$$

TABLE III. Total energies for heavy ions (singly ionized) from the relativistic SCF and the relativistic semistatistical model.

Z	Energy (keV) $-E_{RSCF}$	$-E_{RW}$ [a]	$-E_{RT}$ [b]
87	661.1	616.8	727.0
79	517.6	482.5	559.9
55	211.6	195.0	221.1
47	144.7	132.2	149.6
37	80.90	73.26	83.07
29	44.87	40.17	45.82

[a]This energy is obtained using $\epsilon_{RW}(x)$ for $x < x_0$ and $\epsilon_{RT}(x)$ for $x > x_0$.

[b]This energy is obtained using $\epsilon_{RT}(x)$ over the entire range of x.

The boundary point x_0 is obtained from the conditions $\epsilon_{RT}(x_0) = \epsilon_{RW}(x_0)$, using Eqs. (41) and (45).

The nonrelativistic limits ($\alpha \to 0$) in all of the above expressions agree with their nonrelativistic counterparts in Sec. III.

The results for total atomic binding energies for heavy singly ionized atoms are presented in Table III. The results are compared to the relativistic self-consistent-field (RSCF) energies (E_{RSCF}) by Barnes and Cowan.[25] The atomic binding energy from the statistical method may be calculated in two ways. First, an energy denoted by E_{RW} is calculated[26] using $\epsilon_{RT}(x)$ for $x < x_0$; secondly, an energy denoted by E_{RT} is calculated[26] using $\epsilon_{RT}(x)$ for $x < x_0$. $\epsilon_{RT}(x)$ is used in both calculations for all $x \geq x_0$. The energies E_{RW} are 6% higher than E_{RSCF} for Fr^+ ($Z = 87$) increasing to 11% higher for Cu^+($Z = 29$). This error range is the same as the corresponding calculation using the nonrelativistic semistatistical model. The energy E_{RT} is not as good in comparison to the respective nonrelativistic case; here the energy is low by 10% for Fr^+ and by 2% for Cu^+. By comparing the difference in energy between the nonrelativistic and relativistic semistatistical models to the corresponding SCF energy difference in Fig. 8, we observe that $E_W - E_{RW}$ is off by 13% to 8%, depending upon Z, whereas $E_T - E_{RT}$ is roughly 100% off. It appears that the relativistic semistatistical model (using the wave mechanical formula to calculate the energy for $x < x_0$) gives a good qualitative account of relativistic effects in complex atoms.

In Table IV, some specific results are listed. We note that relativistic effects cause x_0 to decrease in comparison to the nonrelativistic calculation, and further, since the charge cloud is pulled in tighter, the potential of the nucleus is greatly affected for large Z. In Fig. 9, a comparison is made between the relativistic and nonrelativistic radial charge densities for Fr^+. This effect is one order of magnitude greater than the Dirac exchange correction to the TF model. The Dirac exchange energy for $Z = 80$ is approximately[27] 5 keV (Table V) and only slightly influences the shape of the TF density.[28]

A problem arises with the relativistic semistatistical model for values of Z greater than 86. As Z increases, the matching boundary point x_0 gets so small that $\rho_{RT}(x)$ goes through an inflection and the second derivative becomes positive.[29] As a result, the boundary conditions obtained by matching to $\rho_{RW}(x)$ are not compatible. This phenomenon is reflected in the values of β (see Table IV). We should expect β to be, roughly, slightly less than twice the effective nuclear charge seen by a

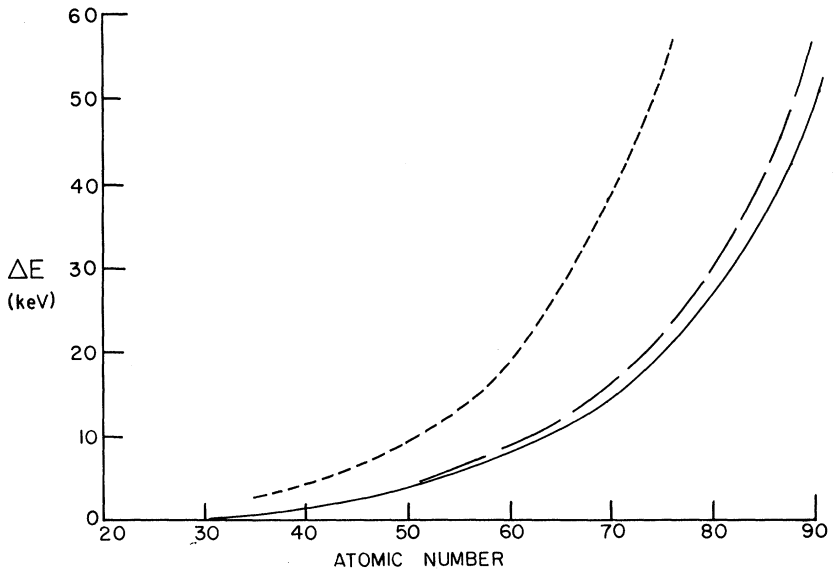

FIG. 8. The difference of total energy between nonrelativistic and relativistic calculations of the semistatistical model. $E_W - E_{RW}$, solid line (E_W and E_{RW} are the total energies calculated from the wave-mechanical energy densities for $x < x_0$ using, respectively, the nonrelativistic and relativistic formulas); $E_{SCF} - E_{RSCF}$ long dashed line. (E_{SCF} and E_{RSCF} are, respectively, the nonrelativistic and relativistic self-consistent-field total energies); $E_T - E_{RT}$ short dashed line (E_T and E_{RT} are calculated using, respectively, the nonrelativistic and relativistic statistical energy densities for $x < x$).

TABLE IV. Results of the relativistic and nonrelativistic semistatistical models for specific singly ionized ions.

Z	x_0	$v_e(0)$ [a]	β	$C(\times 10^5)$	β [b]	C [b] $(\times 10^5)$
87	0.0082	693.2	176.2	7.64	162.6	44.85
79	0.0095	585.6	158.2	8.91	147.4	33.29
55	0.0151	327.9	106.0	6.80	101.8	10.82
47	0.0182	258.2	89.3	4.90	86.7	6.63
37	0.0239	180.8	69.0	2.67	67.8	3.13
29	0.0316	126.2	53.24	1.33	52.61	1.44

[a] See Table II for corresponding nonrelativistic values.
[b] Nonrelativistic.

K electron. This is not the case if Z becomes too large.

V. DISCUSSION

The possibility of using Rudjkobing's density [Eq. (29)] in place of the relativistic TF density [Eq. (28)] for the semistatistical model has been investigated. It was found that the additional term $[r(dV/dr)]^2$ subtracts out most of the relativistic effect on the density. The density curves are very close to those of the nonrelativistic semistatistical model. However, as in the nonrelativistic case, the energies E_{RT} and E_{RW} agree to the corresponding RSCF calculation, with the error range being approximately the same as in the corresponding nonrelativistic calculation. These results are presented in Table VI. In this manner the problem encountered for $Z \geq 87$ is eliminated; however, here the values of β are too small.

Many authors have proposed modifications of the equations of the TF theory in order to arrive at good total energies. Judgment of the quality of these calculations is based strictly on the comparison with wave-mechanical calculations. In the present work, it is apparent that we can obtain good total energies (both relativistically and nonrelativistically) depending on the method of calculation. These energies, even though they might be reasonably accurate, cannot be considered as too significant because the energy densities from which they are obtained differ significantly from the corresponding wave-mechanical-energy densities. Useful calculations from the semistatistical theories might involve calculations of relative differences, such as those compared in Fig. 8.

Beck[30] has used the relativistic semistatistical potential to study relativistic effects on the optical levels of Tl II. Excellent results were achieved for the ground state (i.e., 0.15% error) and excited states of the same J and parity values. The

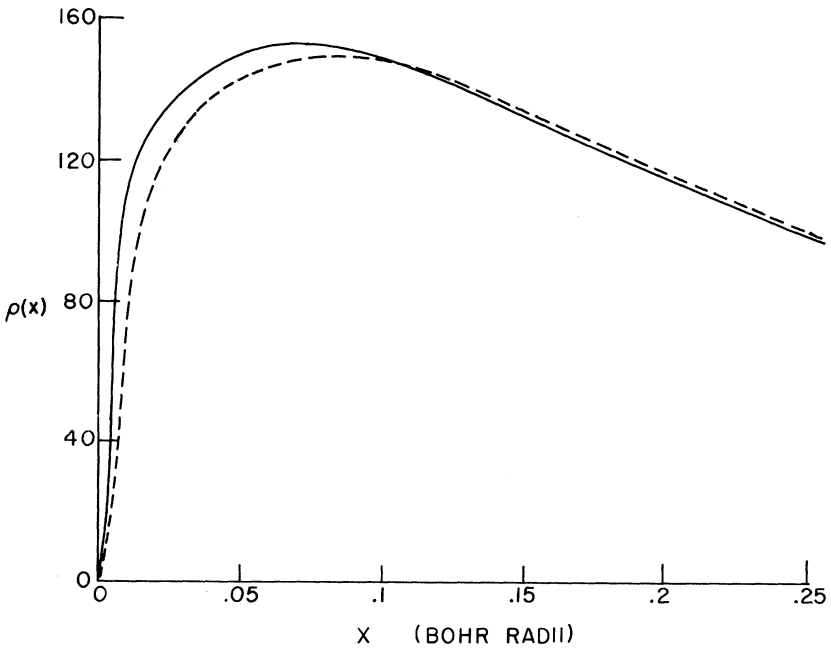

FIG. 9. Comparison of the relativistic and nonrelativistic radial densities for singly ionized francium ($Z=87$) using the semistatistical model. RTF, solid line; RSS, dashed line.

TABLE V. Kinetic, electronic, nuclear-Coulomb energies from the semistatistical [relativistic (RS) and nonrelativistic (NRS)] and Thomas-Fermi (TF) models.

	Kinetic			Electronic			Nuclear Coulomb		
Z	TF	NRS [a]	RS [a]	TF	NRS	RS	TF	NRS	RS
87	702.1	581.2	778.5	233.5	232.8	245.7	−1637.6	−1387.6	−1641.0
79	560.2	460.9	582.4	186.4	185.8	193.9	−1306.8	−1101.3	−1258.8
55	240.6	192.2	214.5	79.97	79.50	81.23	−561.6	−461.2	−490.7
47	166.8	131.3	142.2	55.38	54.96	55.88	−388.9	−315.73	−330.27
37	95.43	73.33	79.09	31.64	31.32	31.66	−222.5	−176.9	−182.0
29	54.05	40.39	41.67	17.88	17.63	17.76	−125.98	−97.88	−99.6
19	20.15	14.21		6.62	6.47		−46.92	−34.74	
11	5.63	3.60		1.82	1.74		−13.07	−8.93	
3	0.2681			0.0700			−0.6062		

[a] This energy is calculated using the wave-mechanical kinetic-energy-density formulas for $x < x_0$.

results for other excited states were poor (partially attributed to neglecting exchange). This is not an unusual phenomenon because it is well known that a universal potential for an atom does not exist. This calculation was based on the low-Z Pauli approximation using configuration interaction with the basis set generated by the relativistic semistatistical potential.

We have used the nonrelativistic semistatistical potential as a given effective one-particle potential for straightforward solution of the Schrödinger equation for all the levels in Cu II up to the third level. Energy eigenvalues for the lowest two states agree to within 5% with HFS calculations. The probability density agrees extremely well with the density obtained from HSCF calculations. This improvement in the one-electron potential is due in part to the fact that in this model the electron density near the nucleus is reduced to a realistic value. The density is then forced by the boundary conditions at x_0 to peak more highly and then drop off more rapidly at large r. This results in a more compact electron cloud and a better one-electron potential than in the TF model.

Thus, the self-consistent semistatistical potentials calculated by means of the models discussed in this paper appear to provide a good starting point for more sophisticated calculations of atomic wave functions.

TABLE VI. Results of the relativistic semistatistical model using Eq. (29) to represent the statistical density. [a]

Z	$-E_{RW}$	$-E_{RT}$	$v_e(0)$	β	x_0
87	609.16	654.88	578.73	131.56	0.0103
79	479.36	517.46	506.68	122.98	0.0113
55	195.46	214.27	306.11	92.42	0.0163
47	132.56	146.32	245.49	80.58	0.0192
37	73.46	81.96	175.04	64.70	0.0248
29	40.27	45.45	123.71	51.18	0.0323

[a] See Tables III and IV for definition of terms.

APPENDIX: NUMERICAL SOLUTION OF THE SELF-CONSISTENT INTEGRAL EQUATION FOR THE DENSITY

In this Appendix we obtain a simple method for integrating Eq. (6). By using a trapezoidal integration technique, it is easy to show that

$$\frac{1}{x}\int_0^x \rho(x')\,dx' = \frac{1}{2x_n}\sum_{i=1}^{n}(\rho_{i-1}+\rho_i)\Delta x_i + \frac{1}{x}\int_0^{\epsilon}\rho(x')\,dx',$$

$$\int_0^x \frac{\rho(x')}{x'}dx' = \frac{1}{2}\sum_{i=1}^{n}\left(\frac{\rho_{i-1}}{x_{i-1}}+\frac{\rho_i}{x_i}\right)\Delta x_i + \int_0^{\epsilon}\frac{\rho(x')}{x'}\,dx', \tag{A1}$$

where $\Delta x_i = x_i - x_{i-1}$, $x_0 = \epsilon$; $\rho_i = \rho(x_i)$, $x_n = x$.

We choose the lower limit for the numerical integration at ϵ, which is some small finite value of x, in order to avoid the singular factor $1/x$ at the origin. The values of the integrals up to ϵ may be analytically determined because the behavior of the density is known for small x.[31] Subtracting the second of Eqs. (A1) from the first gives

$$\int_0^x\left(\frac{1}{x}-\frac{1}{x'}\right)\rho(x')\,dx' = \frac{1}{2x_n}\sum_{i=1}^{n-1}(\rho_{i-1}+\rho_i)\Delta x_i - \frac{1}{2}\sum_{i=1}^{n-1}\left(\frac{\rho_{i-1}}{x_{i-1}}+\frac{\rho_i}{x_i}\right)\Delta x_i - \tfrac{1}{2}(\Delta x_n)^2\frac{1}{x_n x_{n-1}}\rho_{n-1} + \Phi(\xi,\epsilon), \tag{A2}$$

where $$\Phi(\xi,\epsilon) = \int_0^{\epsilon}\left(\frac{1}{x}-\frac{1}{x'}\right)\rho(x')\,dx' \quad . \tag{A3}$$

Substitution of Eq. (A2) into (6) gives

$$\rho_n = \frac{8\sqrt{2}}{3\pi}x_n^{\,2}\left[\xi - \Phi(\xi,\epsilon) + \frac{Z}{x_n} - \sum_{i=1}^{n-1}\left(\frac{1}{x_n}(\rho_{i-1}+\rho_i) - \frac{\rho_{i-1}}{x_{i-1}} - \frac{\rho_i}{x_i}\right)\frac{\Delta x_i}{2} + \tfrac{1}{2}(\Delta x_n)^2\frac{1}{x_n x_{n-1}}\rho_{n-1}\right]^{3/2} \tag{A4}$$

The value of $\rho(x)$ at $x = x_0$ is determined by

$$\rho_0 = (8\sqrt{2}/3\pi)x_0^{\,2}[\xi - \Phi(\xi,\epsilon) + Z/\epsilon]^{3/2} \ ; \tag{A5}$$

hence $\rho_1 = (8\sqrt{2}/3\pi)x_1^{\,2}[\xi - \Phi(\xi,\epsilon) + Z/x_1 + \frac{1}{2}(\Delta x_1)^2(1/x_1x_0)\rho_0]^{3/2}$, etc. (A6)

The convenience of this method is due to the fact that the interaction integral (A2) is completely determined by the known density at the points x_{n-1}, x_{n-2}, etc., and the definite integral $\int_0^{\infty}[\rho(x)/x]dx$ occurs only in the parameter ξ which is adjusted for normalization. Since at each point the density is uniquely determined by the previous values, the self-consistent numerical integration becomes extremely simple. A value for ξ is guessed, the integration for ρ is carried out, and then the integral $\int\rho\,dx$ is checked for correct normalization. The correct value for ξ is then obtained by trial and error; however, the process converges very rapidly.

The solutions are insensitive to the choice of ϵ as long as it remains in the region between 10^{-4} and 10^{-2} Bohr radii. The reason for this is that for radii less than 10^{-4} Bohr radii the numerical integration fails because the function $\rho(x)/x$ is singular; for the region greater than 10^{-2} Bohr radii the analytic form $\Phi(\xi,\epsilon)$, which is obtained by assuming x is small, is no longer sufficiently accurate.

---

*Supported in part by Office of Aerospace Research, under Contract No. A33(615)1652, Applied Mathematics Division, Wright-Patterson Air Force Base, Ohio, through PEC Research Associates, Louisville, Colo.

[1]Literature, up to 1956, can be found in the article by P. Gombás, in Handbuch der Physik, edited by S. Flügge

(Springer-Verlag, Berlin, 1956), Vol. 36.

[2]N. H. March, Advan. Phys. 6, 1 (1957).

[3]E. M. Corson, Perturbation Methods in the Quantum Mechanics of n-Electron Systems (Hafner Publishing Co., New York, 1951), p. 157.

[4]P. Gombás, Rev. Mod. Phys. 35, 512 (1963).

[5]C. F. von Weizsäcker, Z. Physik 96, 431 (1935).

[6]A review with further references on the Weizsäcker correction is given in Ref. 2, p. 80.

[7]K. Yonei and Y. Tomishima, J. Phys. Soc. Japan 20, 1051 (1965).

[8]D. A. Kirzhnits, Zh. Eksperim. i Teor. Fiz. 32, 115 (1957) [English transl.: Soviet Phys. – JETP 5, 64 (1957)].

[9]S. Golden, Phys. Rev. 105, 604 (1957); 107, 1283 (1957).

[10]G. A. Baraff and S. Borowitz, Phys. Rev. 121, 1704 (1961).

[11]H. M. Schey and J. L. Schwartz, Phys. Rev. 137, A709 (1965).

[12]J. S. Plaskett, Proc. Phys. Soc. (London) 66A, 178 (1953).

[13]N. H. March and J. S. Plaskett, Proc. Roy. Soc. (London) A235, 419 (1959).

[14]S. Kobayashi, J. Phys. Soc. Japan 14, 1039 (1959).

[15]H. Brudner and S. Borowitz, Phys. Rev. 120, 2053 (1960).

[16]E. C. Snow, J. M. Canfield, and J. T. Waber, Phys. Rev. 135, 969 (1964).

[17]W. C. Dickinson, Phys. Rev. 80, 563 (1950).

[18]J. F. Barnes and R. D. Cowan, Phys. Rev. 132, 236 (1963).

[19]M. Rudjkobing, Kgl. Danske Videnskab. Selskab, Mat.-Fys. Medd. 27, No. 5 (1952).

[20]J. J. Gilvarry, Phys. Rev. 95, 71 (1954).

[21]G. Temple, Proc. Roy. Soc. (London) A145, 344 (1934).

[22]This wave function is for the spin-up case; however, since we are concerned only with charge densities, it does not matter which wave function we use to obtain the K-electron density.

[23]Only in the nonrelativistic limit does the parameter μ on the right-hand side of this expression become equivalent to its respective nonrelativistic counterpart.

[24]The β in this equation is not to be confused with the β defined by Eq. (41). Here it is the 4×4 matrix,

$$\beta=\begin{pmatrix}1&0&0&0\\0&1&0&0\\0&0&-1&0\\0&0&0&-1\end{pmatrix}.$$

[25]See Ref. 23. These results have been confirmed by A. Rosen and I. Lindgren, Phys. Rev. 176, 114 (1968) by using a modified Hartree-Fock-Slater method.

[26]The potential-energy density

$$-(Z/x)\rho(x)+\tfrac{1}{2}\int dx'[\rho(x')\rho(x)/(x,x')_{>}]$$

is included in addition to kinetic-energy density.

[27]This number is based on a solution to the Thomas-Fermi-Dirac model using the numerical methods presented in Sec. II. Furthermore, the exchange energy is roughly one order of magnitude less than the direct electronic interaction energy. The total energies for our specific ions are broken up into their respective parts in Table V.

[28]N. H. March, Phil. Mag. 44, 1193 (1953).

[29]The matching point x_0 for $Z=87$ is, in fact, slightly inside the inflection point of $\rho_{\mathrm{RT}}(x)$.

[30]D. R. Beck, J. Chem. Phys. (to be published).

[31]The zeroth-order analytic approximation for $\rho(x)$ near the nucleus may be obtained by neglecting

$$\int_0^x(1/x-1/x')\rho(x')\,dx'$$

in Eq. (6). Higher-order terms can be included by binomial expansion of Eq. (6) using the zeroth-order expression to evaluate the above integral.